

07.2

Quantum-cascade lasers based on an active region with low sensitivity to thickness fluctuations

© A.V. Babichev¹, E.S. Kolodeznyi¹, D.A. Mikhailov², V.V. Dudelev², A.G. Gladyshev¹,
S.O. Slipchenko², A.V. Lyutetskii², L.Ya. Karachinsky¹, I.I. Novikov¹,
G.S. Sokolovskii², N.A. Pikhtin², A.Yu. Egorov¹

¹ ITMO University, St. Petersburg, Russia

² Ioffe Institute, St. Petersburg, Russia

E-mail: a.babichev@mail.ioffe.ru

Received April 15, 2024

Revised April 27, 2024

Accepted April 27, 2024

The results of the study of ridge quantum-cascade lasers of the $8\mu\text{m}$ spectral range based on the design of the active region with escape from the lower laser level through scattering by a longitudinal optical phonon and subsequent extraction of charge carriers into the injector layers through the miniband are presented. The use of an active region based on 35 periods forming a cascade and the use of InP waveguide claddings with a thickness of $\geq 3.5\mu\text{m}$, along with the use of additional confining InGaAs layers, made it possible to realize effective heat removal from the active region and a high optical confinement factor ($\sim 68\%$). Increasing the injector doping level made it possible to realize a peak output optical power of the order of $\sim 3.6\text{W}$ with a total wall-plug efficiency of about $\sim 6\%$.

Keywords: Superlattices, quantum-cascade laser, molecular-beam epitaxy, metalorganic vapor phase epitaxy, indium phosphide.

DOI: 10.61011/TPL.2024.08.58920.19953

Metalorganic vapor phase epitaxy (MOVPE) allows for large-scale growth (in bulk) of a wide class of heterostructures for optoelectronics. At the same time, an effect associated with temporal instability of precursor fluxes is observed in epitaxy of multi-period (approximately 400–900 layers in the active region) heterostructures of quantum-cascade lasers (QCLs) [1]. The use of ultrasonic systems for monitoring the precursor concentration in real time [1] and QCL active regions with low sensitivity to fluctuations of the layer thickness in different periods of the cascade [2] makes it possible to compensate for this effect. The effects of phase separation [3], surface roughness, and InAlAs composition variations [4–6]) are observed during MOVPE growth of QCLs with an active region based on mechanically stressed heteropairs. In certain cases, the output parameters of the resulting QCLs turn out to be way below the characteristics of their counterparts grown by molecular beam epitaxy (MBE) [4]. Moreover, the maximum value of mechanical stress of active region layers achieved in MPE is significantly higher than the one corresponding to MOVPE.

In long-wavelength QCLs, the effect of over-barrier emission of carriers from the upper laser level into a continuous spectrum is less pronounced than in short-wavelength QCLs. Therefore, active region designs with heteropairs matched in lattice constant are traditionally used in industrial MOVPE production of QCLs operating in the $8\mu\text{m}$ spectral range.

In the present study, we report the results of examination of QCLs of the $8\mu\text{m}$ spectral range based on an $\text{In}_{0.53}\text{Ga}_{0.47}\text{As}/\text{Al}_{0.48}\text{In}_{0.52}\text{As}$ heteropair produced by MBE.

The active region design with low sensitivity to fluctuations of layer thickness in different periods of the cascade was used [2,4,7] with the aim of its subsequent application in MOVPE.

The heterostructure was grown on an indium phosphide (InP) substrate with a crystallographic orientation of $(001) \pm 0.5^\circ$ and a doping level of $(1-3) \cdot 10^{18}\text{cm}^{-3}$. The lower waveguide cladding was formed from an InP layer $3.5\mu\text{m}$ in thickness with silicon impurity concentration $n = 3.0 \cdot 10^{16}\text{cm}^{-3}$. $\text{In}_{0.53}\text{Ga}_{0.47}\text{As}$ layers with a thickness of 250nm ($n = 4.0 \cdot 10^{16}\text{cm}^{-3}$) were used to provide additional confinement of the active region with the purpose of increasing further the optical confinement factor, which reached 68% for this waveguide type. The active region included 35 periods in a cascade and was formed on the basis of a heteropair of $\text{In}_{0.53}\text{Ga}_{0.47}\text{As}/\text{Al}_{0.48}\text{In}_{0.52}\text{As}$ solid solutions. The upper waveguide cladding included InP layers with a thickness of 3500, 500, and 200 nm and a doping level of $n = 3.0 \cdot 10^{16}$, $7.0 \cdot 10^{18}$, and $1.0 \cdot 10^{19}\text{cm}^{-3}$, respectively. A 200-nm-thick $\text{In}_{0.53}\text{Ga}_{0.47}\text{As}$ layer with a doping level of $2.5 \cdot 10^{19}\text{cm}^{-3}$ was used as the contact layer. The entire QCL heterostructure (InP-based waveguide cladding included) described above was grown by MBE.

The schematic diagram of an active region with escape from the lower laser level through scattering off a longitudinal optical phonon and subsequent rapid extraction of charge carriers into the injector layers through the miniband (I) formed by the lower states of the active region layers [4,6,7] is presented in Fig. 1. The calculated quantum

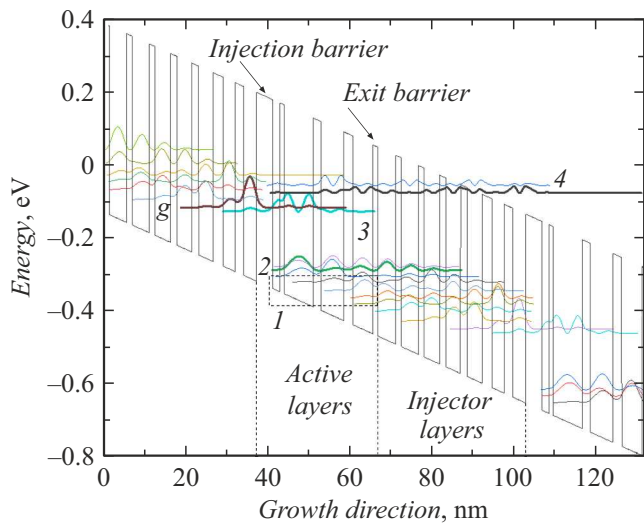


Figure 1. Band diagram of two periods of the active region of the QCL heterostructure (corresponds to an electric field strength of 51 kV/cm). The boundaries of active and injector layers are marked with vertical dotted lines. The boundaries of the miniband are indicated by a dotted rectangle.

energy was 156.3 meV. The significant energy distance (approximately 172 meV) between the lower laser level (2) and the ground injector level (*g*) is indicative of minimization of the parasitic effect of reverse thermal transfer of carriers to lower laser level 2 [7]. The energy distance between the upper laser level (3) and the overlying „parasitic“ level (4) was also increased (to 51 meV), and the spatial overlap of these levels was reduced (to 2.1 nm) in comparison with the design discussed in [6]. The calculated differential gain is slightly higher ($\sim 6\%$) than the value characterizing the design from [6]. In the course of the experiment, we raised additionally the doping level of injector layers (surface concentration $n_s = 2.2 \cdot 10^{11} \text{ cm}^{-2}$) compared to the results presented earlier ($n_s = (1.1-1.5) \cdot 10^{11} \text{ cm}^{-2}$) in [6,8] in order to increase the output optical power of the laser and expand its dynamic range, which is linearly proportional to n_s [9,10].

The QCL crystal was formed in accordance with a procedure similar to the one detailed in [8]. The design used was a deep mesa with a double trench. The depth of etching of the mesa structure was $7.5 \mu\text{m}$. The width of the Fabry–Pérot cavity measured near the surface was $20 \mu\text{m}$. Lasers with a length of 3 mm were studied. QCL crystals were secured with their epitaxial surface onto a copper heat sink using indium solder.

Pulsed current pumping was used to study them at a temperature of 294 K. The pump pulse duration was fixed at 75 ns with a repetition rate of 48 kHz. Lasing spectra were measured with a Bruker Vertex 80v Fourier spectrometer. A Thorlabs PM100/S401C power meter was used to measure the absolute output optical power.

The studied QCLs demonstrated multimode lasing within a wide spectral range ($7.8-8.2 \mu\text{m}$; see the inset in Fig. 2).

Threshold current I_{th} was 2.7 A (this corresponds to threshold current density $j_{th} \sim 4.5 \text{ kA/cm}^2$). Threshold voltage U_{th} determined from the current–voltage curve (Fig. 2) did not exceed 7.6 V. The maximum peak facet output power ($P_{per\text{facet}}$) corresponded to a pump current of $2.6I_{th}$ and was as high as 1.8 W ($P_{total} = 2P_{per\text{facet}} = 3.6 \text{ W}$). The slope of the watt–ampere characteristic corresponding to the facet output power ($SE_{per\text{facet}}$) was 0.67 W/A. The maximum wall plug efficiency (WPE) of the laser (normalized, as in [6], to the doubled facet output power) exceeded 5.9%. These data were compared with the results for MOVPE-grown QCLs of the $8 \mu\text{m}$ spectral range with an active region based on a similar number of periods in a cascade. Record-high output characteristics of QCLs with an active region with escape from the lower laser level through scattering off a longitudinal optical phonon and subsequent rapid extraction of charge carriers into the injector region through the miniband formed by the lower states of the active region layers were reported in [8]. The peak output optical power of ridge QCLs with a stripe contact width of $20 \mu\text{m}$ and a cavity length of 3 mm, which were fabricated based on a heterostructure with 35 periods in a cascade with injector doping level $n_s = 1.1 \cdot 10^{11} \text{ cm}^{-2}$, was two times lower ($P_{per\text{facet}} = 0.9 \text{ W}$ [8]). Notably, these lasers had a steep watt–ampere characteristic (0.8 W/A) and a high maximum WPE ($\sim 9.4\%$) [8]. It has already been demonstrated in [11] that the maximum WPE of a laser increases with a suppression of internal losses in the waveguide, which are directly proportional to the injector doping level. This is consistent with the fact that the experimentally observed efficiency was lower than in [8]. The reduction of internal losses in the waveguide of the studied laser (in comparison with the results presented earlier [8]) from 20 to 11 cm^{-1} was verified by analyzing the slope of the watt–ampere characteristic.

It was demonstrated in [12] that an n_s increase from $1.0 \cdot 10^{11}$ to $2.1 \cdot 10^{11} \text{ cm}^{-2}$ translates into a twofold increase in the output optical power (from 0.46 to 0.93 W) for a laser with a stripe contact width of $24 \mu\text{m}$ and a length of 3 mm. A similar rise of the injector doping level in the studied design (relative to the one discussed earlier in [8]) did also result in a twofold increase in the output optical power.

A comparison was made with the record-high output characteristics of MOVPE-grown QCLs with an active region based on a mechanically stressed heteropair with 35 periods in a cascade. The design of an active region with step quantum wells and barriers was used in [10]; the cascade included 35 periods with the injector layers doped to $n_s = 1.65 \cdot 10^{11} \text{ cm}^{-2}$. Lasers with a stripe contact width of $21 \mu\text{m}$ and a length of 3 mm had similar output optical power levels ($P_{total} = 3.3 \text{ W}$) [10]. The steepness of their watt–ampere characteristic (1.15 W/A) is attributable to the use of a highly reflective coating on the rear facet [10]. In their subsequent studies, the authors of [10] have increased the number of periods in the cascade to 45 and implemented an injector doping level $n_s = 1.0 \cdot 10^{11} \text{ cm}^{-2}$. This increase

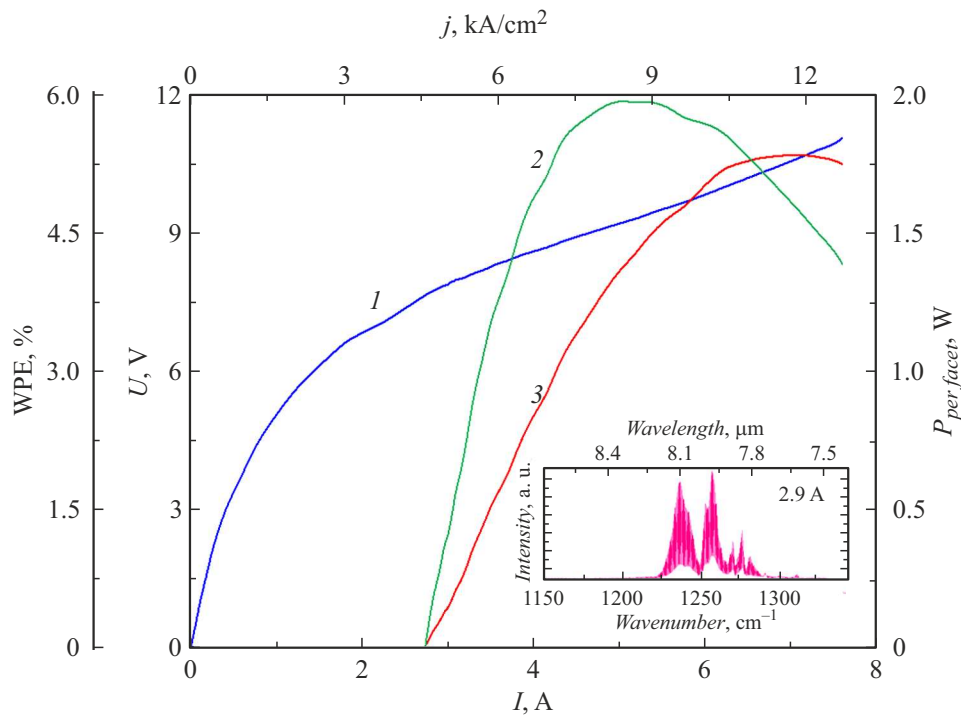


Figure 2. Current–voltage curve (1), dependence of the overall laser efficiency on current (2), and watt–ampere characteristic (3) of the QCL with a Fabry–Pérot cavity. The stripe contact width is $20\ \mu\text{m}$, and the cavity length is 3 mm. The multimode lasing spectrum at a pump current of 2.9 A is shown in the inset.

in the number of periods made it possible to obtain an even steeper watt–ampere characteristic ($2\ \text{W/A}$) due to a reduction in n_s , which affected peak output optical power P_{total} : it did not grow with an increase in the number of cascades, dropping instead to $3.0\ \text{W}$ [13]. These results correspond to a laser with a stripe contact width of $25\ \mu\text{m}$, a length of 3 mm, and a highly reflective coating on the rear facet.

Thus, the results of examination of ridge lasers with an active region with escape from the lower laser level through scattering off a longitudinal optical phonon and subsequent extraction of charge carriers into the injector layers through the miniband formed by the lower states of the active region layers were presented. An output optical power of about $3.6\ \text{W}$ was achieved through the use of this 35-period active region design paired with an efficient waveguide. A twofold increase in output power (compared to the data from [8]) at the cost of a slight reduction in efficiency and steepness of the watt–ampere characteristic of the laser indicates that the discussed QCL design holds much promise for lasers with distributed feedback, including QCLs with a selective ring cavity. These lasers will be the subject of future research.

Acknowledgments

The authors wish to thank B. Schwarz for assistance in calculating the band structure of the QCL active region.

Funding

The examination of laser characteristics performed by researchers from the ITMO University was supported financially by grant No. 20-79-10285–P (<https://rscf.ru/project/20-79-10285/>) from the Russian Science Foundation.

Conflict of interest

The authors declare that they have no conflict of interest.

References

- [1] M. Troccoli, *IEEE J. Sel. Top. Quantum Electron.*, **21** (6), 61 (2015). DOI: 10.1109/JSTQE.2015.2413954
- [2] K. Fujita, S. Furuta, A. Sugiyama, T. Ochiai, T. Edamura, N. Akikusa, M. Yamanishi, H. Kan, *IEEE J. Quantum Electron.*, **46** (5), 683 (2010). DOI: 10.1109/jqe.2010.2048015
- [3] B. Shin, A. Lin, K. Lappo, R.S. Goldman, M.C. Hanna, S. Francoeur, A.G. Norman, A. Mascarenhas, *Appl. Phys. Lett.*, **80** (18), 3292 (2002). DOI: 10.1063/1.1476386
- [4] C.A. Wang, R.K. Huang, A. Goyal, J.P. Donnelly, D.R. Calawa, S.G. Cann, F. O'Donnell, J.J. Plant, L.J. Mis-saggia, G.W. Turner, A. Sanchez-Rubio, *J. Cryst. Growth*, **310** (23), 5191 (2008). DOI: 10.1016/j.jcrysgro.2008.07.100
- [5] R.D. Twesten, D.M. Follstaedt, S.R. Lee, E.D. Jones, J.L. Reno, J.M. Millunchick, A.G. Norman, S.P. Ahrenkiel, A. Mascarenhas, *Phys. Rev. B*, **60** (19), 13619 (1999). DOI: 10.1103/physrevb.60.13619

- [6] B. Schwarz, C.A. Wang, L. Missaggia, T.S. Mansuripur, P. Chevalier, M.K. Connors, D. McNulty, J. Cederberg, G. Strasser, F. Capasso, *ACS Photon.*, **4** (5), 1225 (2017). DOI: 10.1021/acsp Photonics.7b00133
- [7] K. Fujita, S. Furuta, A. Sugiyama, T. Ochiai, T. Edamura, N. Akikusa, M. Yamanishi, H. Kan, *Appl. Phys. Lett.*, **91** (14), 141121 (2007). DOI: 10.1063/1.2795793
- [8] C.A. Wang, B. Schwarz, D.F. Siriani, M.K. Connors, L.J. Missaggia, D.R. Calawa, D. McNulty, A. Akey, M.C. Zheng, J.P. Donnelly, T.S. Mansuripur, F.J. Capasso, *J. Cryst. Growth*, **464**, 215 (2017). DOI: 10.1016/j.jcrysgro.2016.11.029
- [9] Y. Chiu, Y. Dikmelik, P.Q. Liu, N.L. Aung, J.B. Khurgin, C.F. Gmachl, *Appl. Phys. Lett.*, **101** (17), 171117 (2012). DOI: 10.1063/1.4764516
- [10] J.D. Kirch, C.-C. Chang, C. Boyle, L.J. Mawst, D. Lindberg, T. Earles, D. Botez, *Opt. Express*, **24** (21), 24483 (2016). DOI: 10.1364/oe.24.024483
- [11] R. Maulini, A. Lyakh, A. Tsekoun, R. Go, C. Pflügl, L. Diehl, F. Capasso, C.K.N. Patel, *Appl. Phys. Lett.*, **95** (15), 151112 (2009). DOI: 10.1063/1.3246799
- [12] T. Aellen, M. Beck, N. Hoyler, M. Giovannini, J. Faist, *J. Appl. Phys.*, **100** (4), 043101 (2006). DOI: 10.1063/1.2234804
- [13] D. Botez, J.D. Kirch, C. Boyle, K.M. Oresick, C. Sigler, H. Kim, B.B. Knipfer, J.H. Ryu, D. Lindberg, T. Earles, L.J. Mawst, Y.V. Flores, *Opt. Mater. Express*, **8** (5), 1378 (2018). DOI: 10.1364/ome.8.001378

Translated by D.Safin